Performance analysis of Beta-type Stirling cycle refrigerator for different working fluids

Muluken Z. GETIE[1,2,3], Francois LANZETTA[1], Sylvie BEGOT[1], Bimrew T. ADMASSU[3], Steve DJETEL GOTHE[1]

[1]FEMTO-ST Institute, Univ. Bourgogne Franche-Comte, CNRS Parc technologique, 2 avenue Jean Moulin, F-90000 Belfort, France

[2]Bahir Dar energy center, Bahir Dar Institute of Technology, Bahir Dar University, Bahirdar, Ethiopia

[3]Faculty of mechanical and industrial engineering, Bahir Dar Institute of Technology, Bahir Dar University, Bahirdar, Ethiopia

muluken.zegeye@bdu.edu.et (Muluken Z. GETIE)

Abstract: The Stirling cycle refrigerators, which are the counterparts of the Stirling engines are of gas cycle machines. In present paper, experimental investigation and numerical analysis of Beta-type Stirling refrigerator for domestic application are conducted. The refrigeration performances such as input power requirement, cooling power, and coefficient of performance for moderate temperature application have been analyzed using different working fluids (air, nitrogen, helium, and hydrogen). The numerical analysis is conducted to evaluate the perfromence of a machine with respect to different operating frequencies and charging pressures. The result of the analysis showed that air and nitrogen have better cooling power than helium and hydrogen in the operating ranges (15- 25 bar and 6-12 Hz) of the cooling machine. On the other hand, the coefficient of performances in case of helium show higher rate of increase with charging pressure than that of air and nitrogen.

Keywords: Beta type, Experiment, Moderate cooling, Different working fluid, Cooling power

1. Introduction

Recently, due to the limitation of fossil fuels and their environmental impact, researchers in the area of motor have been forced to investigate other types of engines that could replace fossil fuel driven engines. Stirling cycle engine is one of the alternatives as it runs with environmental friendly gases. Stirling cycle machine is a type of external heat engine with a closed thermodynamic cycle. The first Stirling cycle was invented in 1816 by Robert Stirling as a heat engine to convert thermal energy to mechanical energy. The air was used as a working fluid to replace the steam engine since they were prone to life-threatening explosions. By reversing the cycle, the Stirling engine can operate as a heat pump or cooling machine. The Stirling cycle cooling machine, which is the counterpart of the Stirling engine, was first recognized in 1832 [1]. The system was practically realized in 1862, when Alexander Kirk built and patented a closed cycle Stirling refrigerator [2]. Subsequently, different researches have been conducted on Stirling cycle cooling machines and the detailed review is presented in [3].

The configurations of Stirling cycle machines are generally grouped based on piston and piston/displacer-cylinder arrangement as the Alpha, Beta, and Gamma configurations [4,5,6]. All configurations are working with the same thermodynamic cycle but with different mechanical design. Different configuration of Stirling refrigerator have been investigated [7, 8,9,10, 11]. The optimal relation between the cooling rate and the coefficient of performance of the Stirling cycle refrigerating machine was conducted in different researches[12,13,14]. A general analytical model has been introduced for various applications of Stirling refrigerator [15].

The V-type Stirling refrigerator was thermodynamically analyzed [16, 17, 18]. The impact of working fluids on the performance of a V-type Stirling cycle refrigerating machine for a charging pressure less than 5 bar was investigated [17]. The integral V-type Stirling refrigerator was developed, tested, and proven as a domestic cooling machine [18]. The reported COP for such machines varied between 0.1 and 0.9 under different working parameters. The parameters, such as the power demand and the coefficient of performance were examined under different turning speeds and charging pressures. An isothermal model was developed for an Alpha type Stirling cryocooler by considering various losses and the effects of various parameters on cooling performance were investigated [19]. From the research it has been reported that the biggest heat loss was due to conduction loss and the biggest work loss was due to the mechanical friction loss.

Batooei A.et al conducted optimization of a Gamma type Stirling refrigerator based on the experimental and numerical methods [20]. The numerical method applied by this research is multi-objective optimization using non- ideal adiabatic conditions. The cooling capacity and the COP were experimentally investigated for helium and air as a working fluid. The experimental and numerical results from the research proved that the production of cold increases continuously with the speed where the COP has a maximum value. Theoretical and experimental evaluation of the Gamma-type Stirling refrigerator was conducted [21]. The optimum theoretical and experimental analysis coefficients of performances from the research were reported as 0.28 and 0.27 respectively.

Oguz et al. [22] conducted an experimental work for free-piston Stirling coolers. It has been reported that the COP values for coolers operating with warm head temperatures close to 30° C were typically found between 2 and 3 for cold head temperatures around 0° C and falling to around 1 for temperatures approaching -40° C. The effect of parameters such as dead volume ratio, compression ratio, types of working fluids and the phase angle on the performance of a Beta-type refrigerating machine was studied [23]. A 100 W Beta-type Stirling cycle refrigerator was designed and experimentally tested [24]. Hachem et al. developed a thermodynamic model and conducted an experimental validation to optimize air filled Beta-type Stirling refrigeration [25]. Evaluation of the effect of geometrical parameters such as dead space volume and swept volume on the performance of the refrigerating machine was the especial emphasis for this research. A Beta-type Stirling cooler was developed with a rhombic drive system [26]. In the same year the similar configuration Stirling refrigerator was designed and fabricated to achieve a rapid transfer of heat from the system [27]. Helium and carbon dioxide have been used as a working fluid and the more efficient fluid was determined.

Generally, Stirling cycle machines are characterized by high thermal efficiency, low emissions, low vibration, low noise, the ability to use almost every thermal source, low maintenance, safe operation, and reversible working cycle. Furthermore, the findings of most researches done so far proved that Stirling cycle machines are promising alternatives for moderate temperature cooling applications. On the other hand, limited number of researches have been conducted in these types of Stirling cycle refrigerators. Therefore, more studies are needed to enhance the performance of Stirling refrigerators in this application. In the present study, the developed numerical model is validated using an experiment and the effect of working fluid on the refrigerating performance is analyzed for moderate cooling applications. The analysis is conducted for air, nitrogen, helium, and hydrogen at the different operating frequency and charging speed.

2. Mathematical Modeling

2.1. Adiabatic Modeling

A Stirling cycle machine consists of two variable volumes (compression and expansion) spaces at different temperatures and physically separated by a regenerator. For the Stirling cycle refrigerator, heat is absorbed from the low heat source, restore from the regenerator and released the heat to the hot heat exchanger at high temperature and hence store part of heat to the regenerator for the next cycle (see Figure 1). An ideal Stirling refrigeration cycle consists of four separate thermodynamics processes, which consists of two isothermal processes and two constant volume processes as shown in Figure 2.

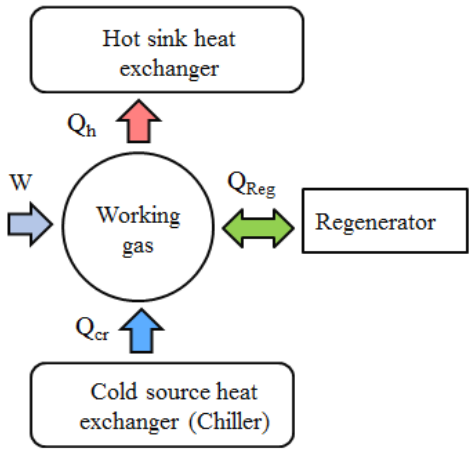

Figure 1. Schematic diagram of Stirling refrigerator

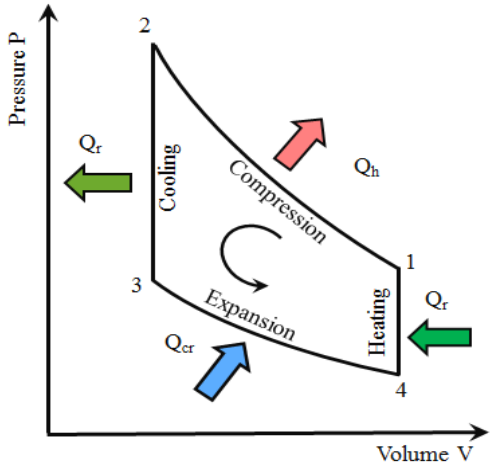

Figure 2. PV- diagram of an ideal Stirling cycle refrigerator

In real Stirling cycle machines, the compression and expansion processes tend to be adiabatic, in which there is no heat transfer to the surroundings. Therefore, the basis of this work is an ideal adiabatic analysis. For easy of analysis, the overall Stirling refrigeration machine is configured into five control volumes (two working spaces and three perfectly effective heat exchangers) serially connected model similarly as described by [6]. The governing equations of the adiabatic equation are shown in Table 1.

Table 1. Governing equations of ideal adiabatic analysis (adapted from [6])

Equation set	Parameter
$dp = \frac{-\gamma P\left(\frac{dV_c}{Tch} + \frac{dV_e}{Tcre}\right)}{\left[\frac{V_c}{TCh} + \gamma\left(\frac{Vh}{Th} + \frac{Vr}{Tr} + \frac{Vcr}{TCr}\right) + \frac{V_e}{Tcre}\right]}$	Pressure change in the system
$dm = \left(\frac{pdV + {Vdp}/{\gamma}}{RT}\right)$	Mass accumulation
$dT = T\left(\frac{dP}{P} + \frac{dV}{V} - \frac{dm}{m}\right)$	Temperature change
$dQ = \frac{VC_v dP}{R} - C_p\,(T_{in}\dot{m}_{in} - T_{out}\dot{m}_{out})$	Heat in three heat exchangers
dW= PdV	work

The ideal adiabatic equation is modified by incorporating shuttle heat loss and gas leakage to the crankcase. This is because these losses have a direct impact on working conditions (pressure and temperature) of working fluid and hence on the overall performance of the machine. So, differential equations of mass and energy conversations of the original ideal adiabatic analysis of the Stirling refrigeration machine has been modified including the effect of mass leakage and shuttle heat losses. Furthermore, the regenerator ineffectiveness loss is included as it has effect on the temperature of the working fluid.

The details of the analysis is presented in [28]. The final equations affected by the mass leakage and shuttle heat loss are presented in equations (1, 2 and 3). The other equations remain unchanged as of the ideal adiabatic model.

$$dp = \frac{-\gamma P\left(\frac{dV_c}{Tch} + \frac{dV_e}{Tcre}\right) + \gamma R\frac{dQ_{shut}}{C_p}\left(\frac{T_{ch} - Tcre}{T_{ch}Tcre}\right) + \gamma R d\dot{m}_{leak}}{\left[\frac{V_c}{TCh} + \gamma\left(\frac{Vh}{Th} + \frac{Vr}{Tr} + \frac{Vcr}{TCr}\right) + \frac{V_e}{Tcre}\right]} \quad (1)$$

$$dm_c = \left(\frac{pdV_c + {V_c dp}/{\gamma}}{RT_{ch}}\right) + \frac{dQ_{shut}}{C_p T_{ch}} \quad (2)$$

$$dm_e = \left(\frac{pdV_e + {V_e dp}/{\gamma}}{RT_{cre}}\right) - \frac{dQ_{shut}}{C_p T_{ch}} \quad (3)$$

2.2. Modified Simple analysis

The heat and power losses that do not have direct impact on the operating condition of a Stirling cycle machine are separately analyzed. These thermal and power losses are assumed as independent to each other and the total losses are the summation of the losses with the respective category. The losses incorporated in modified simple analysis are summarised in Table 2 as developed by the researchers' previous work [28].

Table 2. Summary of losses included in modified simple analysis [28]

No	Types of losses	Equations
1	Heat losses due to internal conduction in the regenerator	$Q_{wrl} = k\frac{A}{L}(Twh - Twcr)$
2	Loss due to regenerator ineffectiveness/external conduction	$Q_{rl} = \dot{m}c_p(1-\varepsilon)(T_c - T_e)$
3	Loss due to pressure drop in heat exchangers	$W_{fr} = \int_0^{2\pi}(\Delta P\frac{dV_e}{d\theta})\,d\theta$ $\Delta P = \Delta p_h + \Delta p_r + \Delta p_{cr}$

4	Heat conduction loss	$Q_{cond} = k\frac{A}{L}\Delta T$
5	Pumping loss	$\dot{Q_p} = (1-\eta)\dot{m}C_p(T_c - T_e)$
6	Loss due to finite speed of piston	$W_{fin-sp} = 2\Delta p_{fin.sp}.V_{swc}$
7	Mechanical Friction loss	$W_{mec.fr} = 2\Delta\, p_{mec.fr}.V_{swc}$
8	Gas Spring hysteresis loss	$W_{gs} = \sqrt{\frac{1}{32}\omega\gamma^3(\gamma-1)T_w P_{mean} Kg}\ (V_d/2V_t)^2 A_w$

3. Experimental setup

The considered experimental device is a reversible thermal machine (motor and/or receiver) with Beta configuration and operates between two constant temperatures. This machine consists of expansion space, heater (acts as a chiller in case of the cooling machine), regenerator, cooler (acts as a hot heat exchanger in case of the cooling machine), compression space, piston, buffer space, and driving mechanisms. The power piston and displacer are arranged within a single cylinder. The displacer piston controls the variations of the expansion volume (cold room) and the power piston controls the compression space (hot room) for such Stirling refrigerating machine. The setup includes a regenerative Stirling refrigerator, cooling water system, the electric supplier, and a data acquisition system. The refrigerator is arranged with six thermometers and one pressure sensor for measuring the working conditions. The setup of the refrigerating machine is demonstrated in Figure 3.

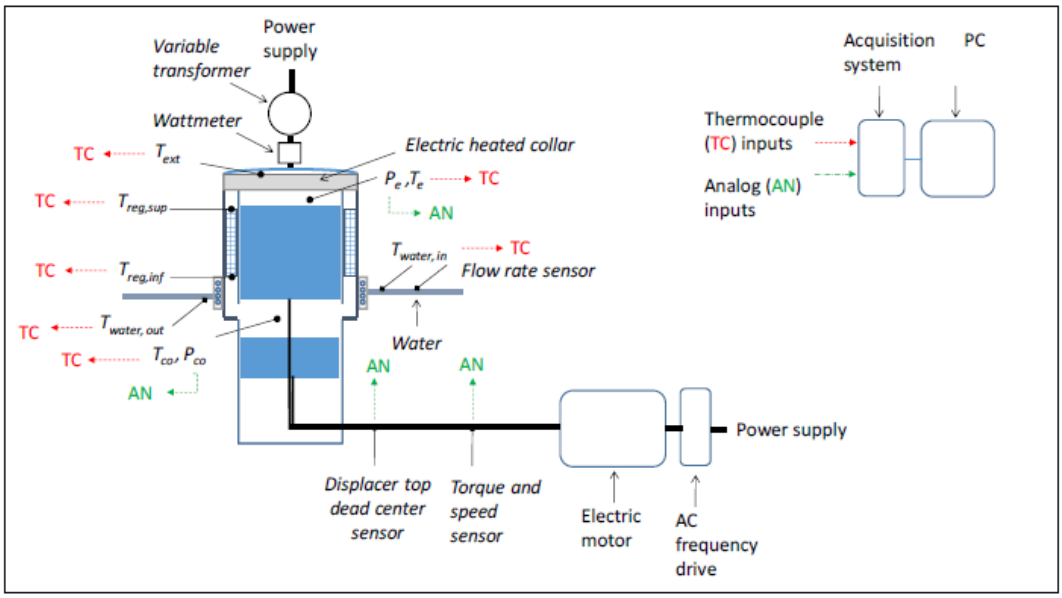

Figure 3. Experimental setup of Stirling refrigerator

The hot heat exchanger and the chiller both have slot geometric arrangement and the configuration of the regenerator is an annular configuration with a stainless steel woven screens matrix. The main parameters and dimensions of the experimental device are shown in Table 3.

The refrigeration rotational speed varied between 435 to 725 rpm and the charging pressure is varied between 15-25 bar. The cooling capacity, coefficient of performance of the refrigerating machine, and minimum achievable no-load temperature of a Stirling refrigerator are determined experimentally. The thermal load was applied to the cold head of the Stirling refrigerator by two resistance heaters in a so-called adiabatic box, and steady-state characteristics of the coolers were evaluated. For a certain input voltage, different tests were carried out to determine the variation of the performance with the cold head temperature, hence the cold head temperature of the coolers varied from -40°C to 0°C. The detail experimental setup is presented in [28,29]. The working gas considered in the experiment is nitrogen, which is assumed to behave like a perfect gas.

Table 3. Experimental engine specification

No	Parameters	value
1	Hot heat temperature (°C)	32
2	Cooling temperature (°C)	-5
3	Piston diameter (mm)	60
4	Displacer diameter (mm)	59
5	Piston stroke (mm)	40
6	Compression space swept volume (cm^3)	103
7	Expansion space swept volume (cm^3)	113
8	Working gas	Nitrogen
9	Frequency (Hz)	7.5
10	Charging pressure (bar)	20

Table 4 illustrates the three experimental result conducted at different electrical input power. In the Table, the electrical power loss, cooling production, the temperature of a gas at the cold side, and coefficent of performance of the machine are presented. As the gas temperature at the cold end increases, both cooling production and COP increases.

Table 4. Experimental result at a charging pressure of 17.5 bar (nitrogen)

Parameters	Experiment 1	Experiment 2	Experiment 3
Electric power (W)	1650	1640	1460
Power loss electrical (W)	285.2	280.5	251
Power mechanical (W)	1365	1359	1209
Cold production (W)	451	554	676
Hot water power (W)	1429	1472	1476
Cooling temperature (°C)	-15.1	-4.3	10.5
Temperature at exit head (°C)	-10	1	16
Speed (rpm)	721	721.8	724
Torque (Nm)	18	18	16
COP (mechanical)	0.33	0.41	0.56

Figure 4 shows a no-load temperature distribution at different parts of the refrigerating machine with Nitrogen as a working gas. Initially, the refrigerator was set at ambient temperature and once the motor is switched on, the temperature of the cold side (expansion space) drops quickly and reaches a steady state cold-end temperature. The minimum no-load temperature achieved at a pressure of 25 bar and a frequency of 12.1 Hz is -68°C. The stabilization temperature is found after 20 minutes of operation. It is recognized that after the machine starts running, the buffer space temperature increases considerably from around 17.4°C to 40°C . This confirms that there is heat loss to the buffer space.

Figure 5 is a plot of temperature variaition versus time in different parts of the refrigerating machine. The experiment was run for 90 minutes to confirm the trend of the cooling process for a long period using nitrogen as a working gas.The stabilization temperature at the cold end is −15.1° C at a cooling load of 451 W, charging pressure of 17.5 bar and frequency of 12.1 Hz. Such Stirling refrigerator needs only 3 minutes to reach such a low temperature and the stabilization temperature is achieved after 40 minutes. The minimum temperature found is −24.9°C and achieved 10 minutes after starting the operation. The buffer space temperature rises approximately by (10° C) from the ambient temperature. This result shows that there seems more gas leakage

towards the buffer space that may result in heat loss. Furthermore, the stabilized temperature difference between the compression space (warm section) and the buffer space is less than $4^{o}C$.

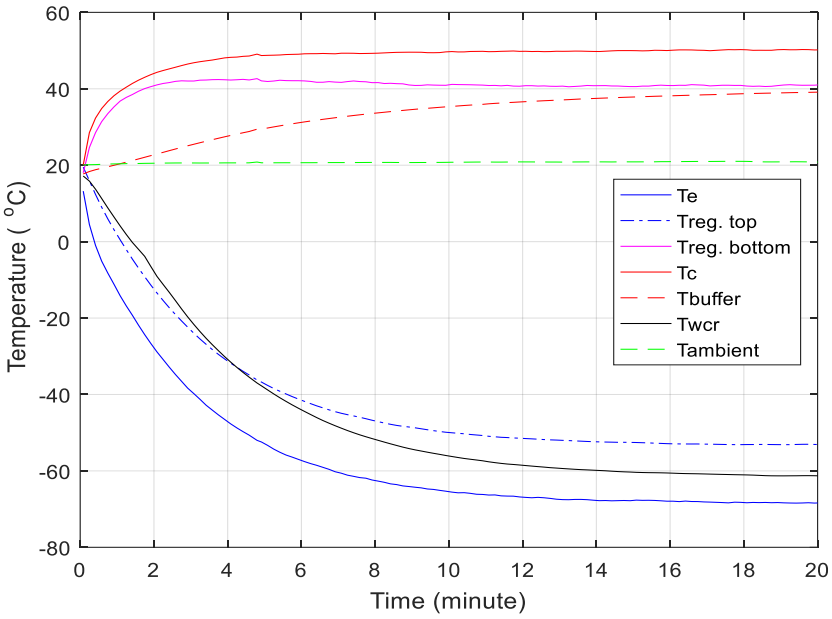

Figure 4. No-load temperature variation at P =25 bar and operating frequency =12.1 Hz

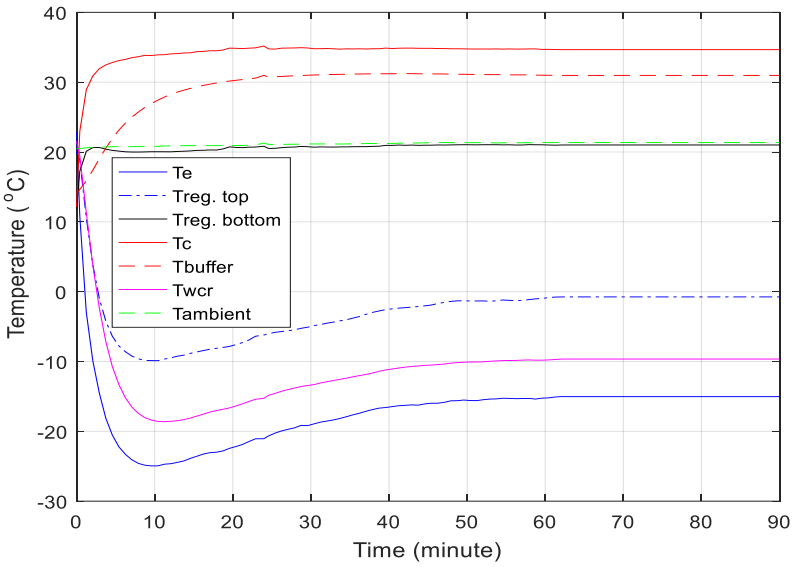

Figure 5. Temperature distribution versus time at P=17.5 bar, operating frequency =12.1 Hz, and cooling load =451 W

As shown in figure 6, the temperature of water in hot heat exchanger increases considerably. The heat power rejected with the flow of water at a hot heat exchanger could be given by the flow rate of water specific heat of the water and the change in temperature of water flowing in this heat exchanger.

$$\dot{Q}_h = \dot{m}_h C_p (T_{h,ex} - T_{h,in}) \tag{4}$$

Where flow of water ($\dot{m}_h$ =3kg/min), C_P = 0.00116kW h/(kg.K), $T_{h,ex}$ is temperature of water at hot heat exchanger exit, and $T_{h,in}$ is temperature of water at entry of hot heat exchanger.

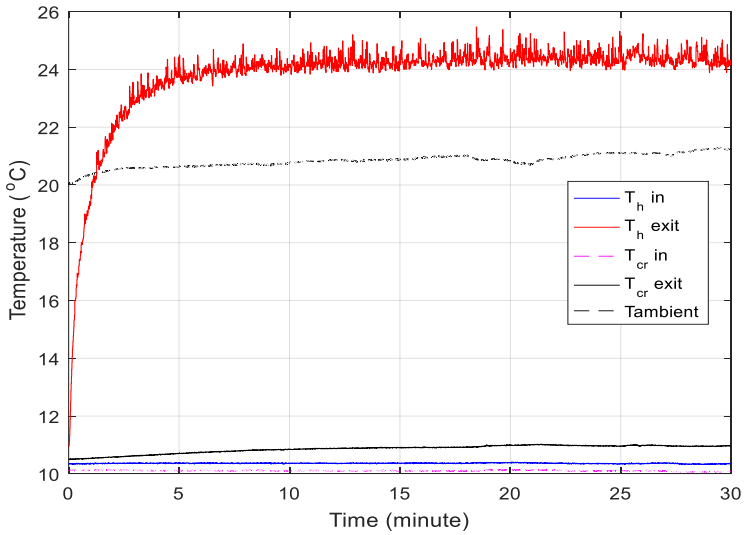

Figure 6.Temperature of working fluid at 25 bar and 12.1 Hz

4. Results and discussion

The numerical model is validated experimentally using the FEMTO 60 Stirling engine as described in the researchers' previous work [28]. In this part of the research, the simulation results of the analysis present the effect of different working fluids (air, helium, hydrogen and nitrogen). The simulation was conducted using these fluids at the different operating frequencies and charging pressures to investigate the cooling performance of the machine.

Figure 7 illustrates the required input power versus operating frequency for different working fluids (air, nitrogen, helium, and hydrogen) at T_h = 27 ºC, T_{cr} = -3 ºC, and a charging pressure of 17.5 bar. It can be observed that the input power requirement increases with operating frequency for all working fluids. Furthermore, it could be seen that air and nitrogen fluids require more input power than helium and hydrogen. These result confirms that air and nitrogen operate at higher flow resistance than helium and hydrogen due to higher mass flow rate.

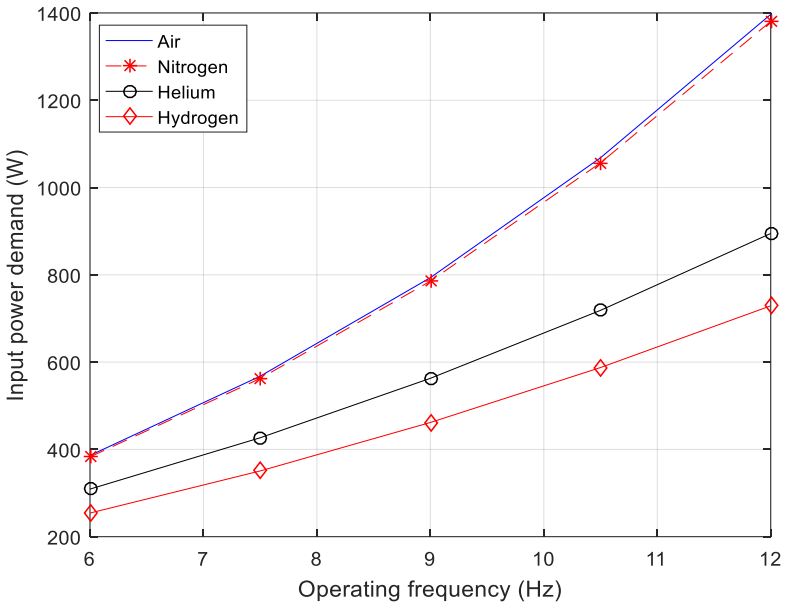

Figure 7. Effect of working fluid fluid on input power requirement of with operating frequency

Figure 8 shows the impact of different working fluids on cooling power with an increase in operating frequency at T_h = 27 ºC, T_{cr} = -3 ºC, and a charging pressure of 17.5 bar. Similar to Figure 7, it can be observed that

the cooling power increases with the operating frequency for all working fluids types. Furthermore, it could be seen that the cooling power for air and nitrogen is more than the cooling power of helium and hydrogen gases. There are two potential reasons for less cooling performance of helium and hydrogen as compared with air and nitrogen. First, the masses of helium and hydrogen are much lower than air and nitrogen, and hence lower heat removal rate as a result lower cooling power. Second, helium and hydrogen have higher thermal conductivity which lead to higher shuttle heat losses and these cause helium and hydrogen gases to produce lower cooling power than air and nitrogen. The shuttle heat loss has a complex effect on affecting the cooling machine performance as it affect the working fluid pressure and temperature.

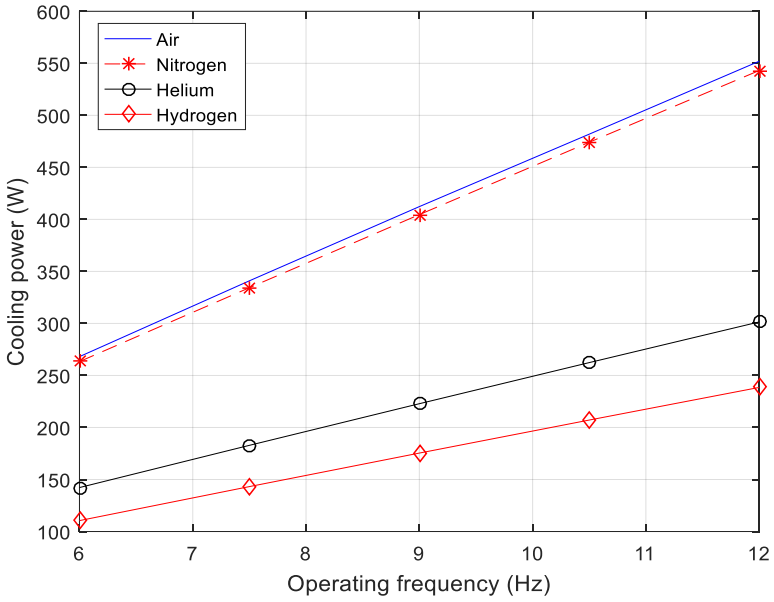

Figure 8. Cooling capacity vs opperating frequency at different working fluid types

Figure 9 demonstrates the effect of different working fluids on the COP of a cooling machine with respect to operating frequency at T_h = 27 °C, T_{cr} = -3 °C, and charging pressure of 17.5 bar. It can be seen that air and nitrogen have better COP than helium and hydrogen within the range of operating frequency. Eventhough, both input power requirement and cooling power increases with operating frequency, COP deareases as a result of higher rate of increase of flow friction and mechanical friction loss. The COP for air and nitrogen deacreases radically with operating speed and this trend shows that at very higher operating speed the COP for helium may be higher than COP of air and nitrogen.

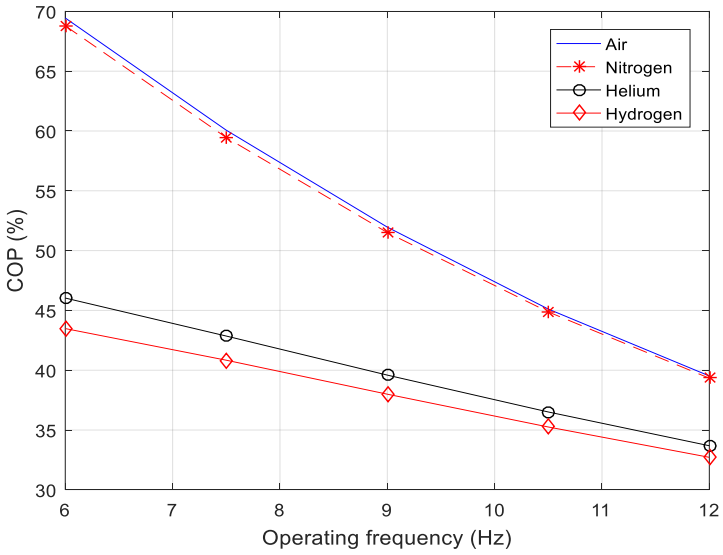

Figure 9. COP vs operating frequency for differnt working fluid types

Figure 10 is a diagram demonstrating the required input power versus charging pressure for different working fluids at T_h = 27 °C, T_{cr} = -3 °C, and an operating frequency of 7.5 Hz. It can be observed that the input power requirement increases with pressure for all working fluids. Furthermore, it could be seen that air and nitrogen fluids require more input power than helium and hydrogen. This is because air and nitrogen operate at higher flow resistance than helium and hydrogen due to higher mass flow rate for a given operating condition.

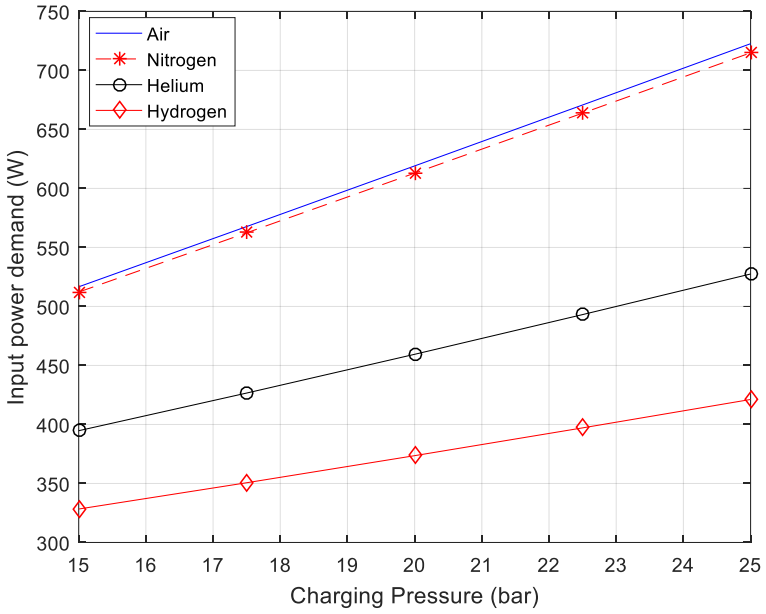

Figure 10. Effect of different fluid types on input power requirement with pressure

Figure 11 displays the influence of working fluids (air, nitrogen, helium, and hydrogen) on cooling power with respect to charging pressure at T_h = 27 °C, T_{cr} = -3 °C, and an operating frequency of 7.5 Hz. It can be observed that the cooling power increases with charging pressure for all working fluids. Furthermore, it could be observed that the cooling power for air and nitrogen is greater than the cooling power of helium and hydrogen due to higher mass flow rate which leads ot higher heat removal rate.

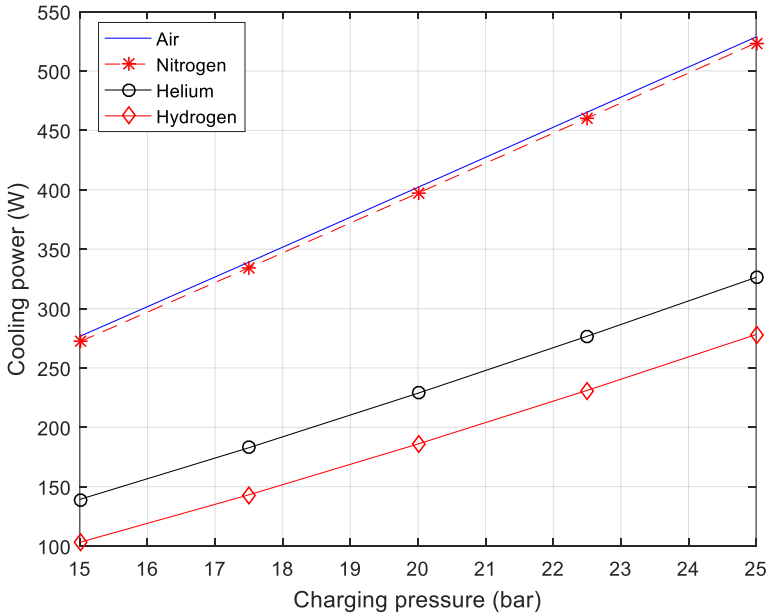

Figure 11. Effect fluid types on cooling capacity of Stirling cycle refrigerator with pressure

Figure 12 displays the influence of working fluids on the COP of the refrigerating machine with charging pressure at T_h = 27 °C, T_{cr} = -3 °C, and an operating frequency of 7.5 bar. Air and nitrogen have by far better COP than helium and hydrogen. The COP for nitrogen increases from 53% to 73% as the charging pressure

increases from 15 bar to 25 bar. The COP for helium increases radically with charging pressure due to lower rate of increasing in flow friction losses as compared with air and nitrogen.

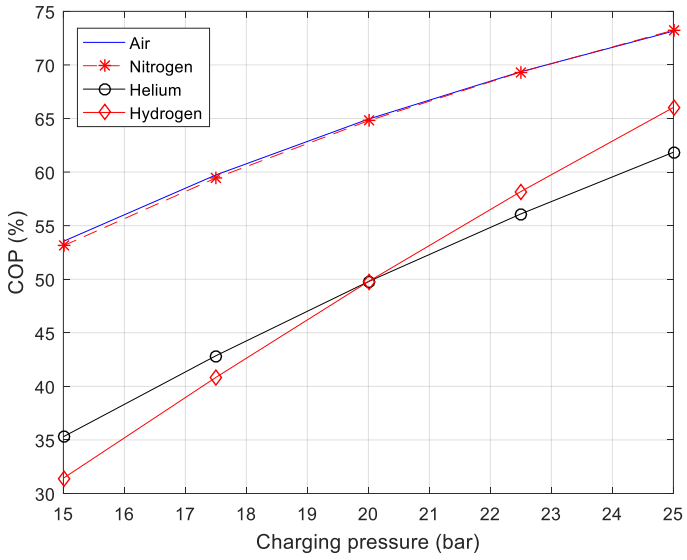

Figure 12. COP vs Charging pressure for different working fluids

5. Conclusion

In this research work, the experimental results are presented with and with out load and performance analysis of the developed model is conducted for domestic cooling applications. The experimental investigation is used to determine the actual cooling power, coefficient of performance of the refrigerating machine, and minimum achievable no-load temperature of a particular Stirling cycle refrigerator. The minimum cold side no-load gas temperature found with experiment at a charging pressure of 25 bar and an operating frequency of 12.1 Hz is -68°C. The perfromance of the cooling machine at different working fluids such as nitrogen, air, helium, and hydrogen are analyzed using the numerical simulation at different operating frequency and charging pressures of the machine within the operating range. Based on the analysis the following results have been found:

- Cooling power and input power required increased with charging pressure and with operating frequency for all considered working fluids for a typical Beta-type Stirling cycle refrigerating machine.
- COP decreases with increase in operating frequency and increases with increasing with charging pressure for all considered working fluids. The trend of COP with respect to operating frequency and charging pressure showed that helium could have better COP at higher pressure and frequency.
- Air and nitrogen have by far higher cooling power than helium and hydrogen due to higher heat removal rate as a result of higher mass flow rate.
- Air, which is easily available gas, could be prefered as a working fluid for domestic Stirling cycle cooling machinedue to a better comparative performance especially in most of the operating ranges (frequency and pressure) of such machine.

Nomenclature

A= cross section area (m2)

Cp= isobaric specfic heat (J.kg-1.K-1)

Cv= isochoric specfic heat (J.kg-1.K-1)
K = heat conductivity ($W.m^{-1}.K^{-1}$)
P = pressure (Pa)

m= mass of working gas (kg)
$\dot{m}$ = mass flow rate (kg/s)
Q= heat (J)
V= volume (m^3)
V_d= instantaneous swept volume of displacer (m^3)
V_{swc}= swept volume of compression (m^3)
R = gas constant ($J.kg^{-1}.K^{-1}$)
T = temperature (K)

W= work (J)

Greek symbols

ε = regenerator effectiveness

η = clearance effciency

γ= ratio of specific heats , (C_p / C_v)

θ= crank angle (°)

ω = omera (rad/s)

subscripts

c = compression space

cr = chiller

e = expansion space

g= gas

h = hot heat exchanger

leak = leakage

mean = mean value

r = regenerator

shut = shuttle

t = total

w = wall

References

1. Kohler, J. W. (1968). The stirling refrigeration cycle in cryogenic technology. The Advancement of Science, 25:261.
2. Kirk, A. C. (1874). On the mechanical production of cold.(includes plates and appendix). In Minutes of the Proceedings of the Institution of Civil Engineers, volume 37, pages 244–282. Thomas Telford-ICE Virtual Library.
3. Getie, M.Z., Lanzetta, F. , Bégot, S., Admassu, B.T., and Hassen A.A. (2020). Reversed regenerative Stirling cycle machine for refrigeration application: a Review. *International Journal of refrigeration, https://doi.org/10.1016/j.ijrefrg.2020.06.007.*
4. Kirkley, D. (1962). Determination of the optimum configuration for a stirling engine. Journal of Mechanical Engineering Science,
5. Reader, G. T. and Hooper, C. (1983). Stirling engines. E. and F. Spon, New York, NY, USA.
6. Urieli, I. and Berchowitz, D. M. (1984). Stirling cycle engine analysis. A. Hilger Bristol.
7. Ahmadi, M. H., Ahmadi, M.-A., Mohammadi, A. H., Mehrpooya, M., and Feidt, M. (2014). Thermodynamic optimization of stirling heat pump based on multiple criteria. Energy Conversion and Management, 80:319–328.
8. De Boer, P. (2011). Optimal performance of regenerative cryocoolers. Cryogenics, 51(2):105–113.
9. Li, R. and Grosu, L. (2017). Parameter effect analysis for a stirling cryocooler. International Journal of Refrigeration, 80:92–105.
10. Tyagi, S., Lin, G., Kaushik, S., and Chen, J. (2004). Thermo economic optimization of an irreversible stirling cryogenic refriger- ator cycle. International journal of refrigeration, 27(8):924–931.
11. Xu, Y., Sun, D., Qiao, X., Yan, S., Zhang, N., Zhang, J., and Cai, Y. (2017). Operating characteristics of a single-stage stirling cryocooler capable of providing 700 w cooling power at 77 k. Cryogenics, 83:78–84.
12. Chen, J. (1998). Minimum power input of irreversible stirling refrigerator for given cooling rate. Energy conversion and management, 39(12):1255–1263.
13. Chen, J. and Yan, Z. (1996). The general performance characteristics of a stirling refrigerator with regenerative losses. Journal of Physics D: Applied Physics, 29(4):987.
14. Razani, A., Dodson, C., and Roberts, T. (2010). A model for exergy analysis and thermodynamic bounds of stirling refrigerators. Cryogenics, 50(4):231–238.
15. Ataer, O¨. E. and Karabulut, H. (2005). Thermodynamic analysis of the v-type stirling-cycle refrigerator. International Journal of Refrigeration, 28(2):183–189.
16. Guo, Y., Chao, Y., Wang, B., Wang, Y., and (2019). A general model of stirling refrigerators and its verification. Energy Conversion and Management, 188:54–65.Gan, Z.
17. Tekin, Y. and Ataer, O. E. (2010). Performance of v-type stirling-cycle refrigerator for different working fluids. International journal of refrigeration, 33(1):12–18.
18. Le'an, S., Yuanyang, Z., Liansheng, L., and Pengcheng, S. (2009). Performance of a prototype Stirling domestic refrigerator. Applied Thermal Engineering, 29 (2-3):210–215.
19. Ahmed, H., Almajri, A. K., Mahmoud, S., Al-Dadah, R., and Ahmad, A. (2017). CFD modelling and parametric study of small scale alpha type stirling cryocooler. Energy Procedia, 142:1668– 1673.
20. Batooei, A. and Keshavarz, A. (2018). A gamma type stirling refrigerator optimization: An experimental and analytical investigation. International Journal of Refrigeration.
21. Katooli, M. H., Moghadam, R. A., and Hajinezhad, A. (2019). Simulation and experimental evaluation of stirling refrigerator for converting electrical/mechanical energy to cold energy. Energy conversion and management, 184:83–90. 4(3):204–212.

22. Oguz, E. , and Ozkadi, F. (2000). An experimental study on the refrigeration capacity and thermal performance of free piston stirling coolers.
23. Otaka, T., Ota, M., Murakami, K., and Sakamoto, M. (2002). Study of performance characteristics of a small stirling refrigerator. Heat TransferAsian Research, 31(5):344–361.
24. Gheith, R., Aloui, F., and Nasrallah, S. (2011). Experimental study of a beta stirling thermal machine type functioning in receiver and engine modes. Journal of Applied Fluid Mechanics, 4:33–42.
25. Hachem, H., Gheith, R., Aloui, F., and Nasrallah, S. B. (2017). Optimization of an air-filled beta type stirling refrigerator. International Journal of Refrigeration, 76:296–312.
26. Cheng, C.-H., Huang, C.-Y., and Yang, H.-S. (2019). Development of a 90-k beta type stirling cooler with rhombic drive mechanism. International Journal of Refrigeration, 98:388–398.
27. Suranjan, S., John, J. S., Mathew, A. J., Jose, J., Joshy, G., Ramesh, A., and Sachidananda, H. (2019). Determination of coefficient of performance of stirling refrigeration sm. International Journal of Innovative Technology and Exploring Engineer ing (IJITEE), 8:2522–2529.
28. Getie, M. Z., Lanzetta, F., Bégot, S., Admmassu, B. T., and Djetel-Gothe, S. (2020). Numerical Modeling and experimental validation of a Beta-type Stirling refrigerator. Submitted for publication.
29. Djetel-Gothe, S., Lanzetta, F., Bégot, S., and Gavignet E. (2020). Design, manufacturing and testing of a Beta Stirling machine for refrigeration applications. International Journal of Refrigeration, 115: 96-106